Prediction of seismic-induced structural damage using artificial neural networks

Oliver Richard de Lautour

Department of Civil and Environmental Engineering

The University of Auckland

New Zealand

Email: oliver.delautour@beca.com

Piotr Omenzetter

Department of Civil and Environmental Engineering

The University of Auckland

Private Bag 92019

Auckland Mail Centre

Auckland 1142

New Zealand

Email: p.omenzetter@auckland.ac.nz

Tel.: +64 9 3737599 ext. 88138

Fax: +64 9 3737462

Abstract

Contemporary methods for estimating the extent of seismic-induced damage to structures include the use of nonlinear finite element method (FEM) and seismic vulnerability curves. FEM is applicable when a small number of predetermined structures is to be assessed but becomes inefficient for larger stocks. Seismic vulnerability curves enable damage estimation for classes of similar structures characterised by a small number of parameters, and typically use only one parameter to describe ground motion. Hence they are unable to extend damage prognosis to wider classes of structures, e.g. buildings with a different number of storeys and/or bays, or capture the full complexity of the relationship between damage and seismic excitation parameters. Motivated by these shortcomings, this study presents a general method for predicting seismic-induced damage using Artificial Neural Networks (ANNs). The approach was to describe both the structure and ground motion using a large number of structural and ground motion properties. The class of structures analysed were 2D reinforced concrete (RC) frames that varied in topology, stiffness, strength and damping, and were subjected to a suite of ground motions. Dynamic structural responses were simulated using nonlinear FEM analysis and damage indices describing the extent of damage calculated. Using the results of the numerical simulations, a mapping between the structural and ground motion properties and the damage indices was than established using an ANN. The performance of the ANN was assessed using several examples and the ANN was found to be capable of successfully predicting damage.

1. Introduction

The ability to assess the vulnerability of civil infrastructure to earthquake-induced damage is undoubtedly one of the most important challenges faced by structural engineers. Two methods are predominantly used for predicting seismic damage: numerical analysis using nonlinear finite element method (FEM) and seismic vulnerability curves. Nonlinear FEM analysis is particularly applicable when a detailed damage estimate is only required for an individual important or typical, representative structure, or a small number of structures [1-4]. However, if an assessment is required for numerous structures the process becomes time consuming and inefficient [5, 6]. Seismic vulnerability curves provide a more efficient method for predicting damage to a class of similar structures. They are generally constructed based on either statistical analysis of field data and historic records [7-13] or analytically simulated data [14-23]. However, these curves typically take into account only a limited number of structural properties and use one parameter to describe ground motion. Hence they have difficulty in extending damage prognosis to wider classes of structures, e.g. buildings with a different number of storeys and/or bays, or capture the full complexity of the relationship between damage and seismic excitation parameters [6, 24]. This shortcoming becomes particularly important as studies [25, 26] have shown that correlations between damage and the parameters describing ground motion are very complex and a set of such parameters rather than one index would be necessary to capture the relationships.

These shortcomings stimulated research into more general methods and models capable of extending damage prediction to larger classes of structures and incorporating a wider set of parameters describing ground motions. However, research into such methods appears to be still scarce. Several authors attempted to extend the usability of vulnerability curves. Kwon and Elnashai [6] observed large variability of vulnerability curves for a single RC frame and calculated three different vulnerability curves for sets of ground motions with different peak ground acceleration to peak ground velocity ratios. Using extensive numerical simulations of single degree of freedom nonlinear oscillators characterized by period, strength, ductility and post-yield stiffness, Jeong and Elnashai [5] built a data base which could later be used to retrieve information and construct vulnerability curves faster. Serdar Kircil and Polat [24] used a statistical method to combine vulnerability curves for the same RC building constructed with two alternative reinforcement grades and later used regression analysis to extend their curves to buildings with a different number of storeys. From these examples it can be seen that work on generalization of damage prediction to different structures and ground motion within the framework of traditional vulnerability analysis has started but still poses a significant challenge. The use of discriminant analysis is reported by Yücemen et al. [27], who predicted building damage into a two-state or three-state damage classification. The analysis was based on post-earthquake data from the Turkish 1999 Duzce earthquake. Three structural parameters were found to discriminate the data set the most: the number of storeys, a ratio of the ground storey height to the first storey height and a ratio of the column area to the floor area. Yakut et al. [28] extended this approach and considered also local soil characteristics.

A tool that is often used to describe complex relationships influenced by numerous parameters are Artificial Neural Networks (ANNs). Although ANNs have been applied widely throughout the civil engineering [29] and structural health monitoring fields [30-32], their use for seismic damage prediction has been limited. Molas and Yamazaki [33] used an ANN to predict seismic damage in wooden framed houses represented by simple analytical single degree of freedom models. In the study, ground motion indices were related to structural ductility using the ANN. De Stefano et al. [34] described an approach to predict seismic damage mechanisms in historic churches using an ANN and Bayesian classification. The church was broken into different structural components, e.g. facade, apse, sidewalls, spire etc. These components and their arrangement were used as ANN input. The ANN was used to give the probability of each damage mechanism occurring. A similar approach was used by Aoki et al. [35] to predict the seismic collapse mechanisms in chemical plants. Erkus [36] used ANNs to predict seismic damage in analytical models of reinforced concrete (RC) frame structures. The author was able to predict damage in the frame with varying stiffness and reinforcement ratio whilst under different scaled ground motion intensities. However, no attempt was made to further extend the study to frames with different topologies, i.e. different number of storeys/bays and dimensions. Sánchez-Silva and García [37] proposed using a combination of systems theory, fuzzy logic and ANNs to assess the seismic damage in a structure. Fuzzy logic converted linguistic terms describing the earthquake severity, soil conditions and structural properties into numbers, which were the inputs into an ANN. The system was trained for several types of structures.

In this study, a method for predicting seismic-induced damage using ANNs is proposed that can be applied to a wider class of structures subjected to varying ground motions. The approach was to describe both the structure and ground motion using a number of structural and ground motion properties, thus allowing a wide range of situations to be described. The class of structures analysed were 2D RC frames that varied in topology, stiffness, strength and damping, and were subjected to a suite of ground motions characterized by their Peak Ground Acceleration (PGA), Velocity (PGV) and Displacement (PGD), Spectrum Intensity (SI), dominant frequency and duration. Dynamic structural responses were simulated using nonlinear FEM analysis and damage indices describing the extent of damage calculated. Using the results of the numerical simulations, a mapping between the structural and ground motion properties and the damage indices was then established using an ANN. The efficiency of the ANN for damage prediction was assessed using several examples illustrating the ability to extend damage prognosis.

2. Artificial Neural Networks

ANNs are structures deliberately designed to mimic and utilise the organisational principles observed in the brain [38]. ANNs are capable of efficiently performing tasks such as pattern recognition, classification and function approximation. Adeli [29] gives a comprehensive review of ANN applications in civil engineering.

ANNs utilising the supervised error Back-Propagation (BP) algorithm [39] are commonly referred to as BP neural networks. BP networks appear to be the most popular type of neural network employed. The structure of a BP network with a single hidden layer (HL) is shown in Figure 1, where **x** and **o** are the input and output vectors of the network, respectively. The bias inputs into the HL and output layer (OL) have been represented by solid squares and both have the value of +1. The weights, denoted by vector **w**, are learnt during network training and store information about the processing of input data.

The basic function of a neuron, in either the HL(s) or OL, is to calculate the weighted sum of all inputs u and compute the output y. The weighted sum of all inputs can be calculated as follows:

$$u = \mathbf{v}^T \mathbf{z} \tag{1}$$

where superscript T denotes transposition. The input and weights vectors have been denoted by $\mathbf{v}$ and $\mathbf{z}$ to avoid confusion with $\mathbf{w}$ and $\mathbf{x}$, which are for the whole network. The output of the neuron is computed using

$$y = f(u) \tag{2}$$

where f is the neuron's activation function. Activations functions may have different forms; in this study, the tangent hyperbolic function was used.

When an ANN is to be used as a function approximator, the error between the target values and the network outputs needs to be minimised. In the vector notation, this error can be written as

$$\mathbf{e}(\mathbf{w}) = \mathbf{d} - \mathbf{o}(\mathbf{w}) \tag{3}$$

where $\mathbf{d}$ is the vector of desired network outputs or target values. The total approximation error $E(\mathbf{w})$ is a function of the weights and can be written as

$$E(\mathbf{w}) = \frac{1}{2}\mathbf{e}(\mathbf{w})^T \mathbf{e}(\mathbf{w}) \tag{4}$$

In the training phase, an input selected from a set of known input-output pairs is supplied, and the network calculates the output from the given input. The error between the desired and actual output is then propagated backwards from the output layer to the preceding layers –

hence the name "back-propagation algorithm". In this study, the Levenberg-Marquardt algorithm [40, 41] is used to minimise the error.

Introducing the Jacobian matrix **J** defined by

$$\mathbf{J}(\mathbf{w}) = \frac{\partial \mathbf{e}}{\partial \mathbf{w}} \tag{5}$$

the new weights can be computed iteratively using the following formula:

$$\mathbf{w}_{k+1} = \mathbf{w}_k - \left[\mathbf{J}^T(\mathbf{w}_k)\mathbf{J}(\mathbf{w}_k) + \lambda_k \mathbf{I}\right]^{-1} \mathbf{J}^T(\mathbf{w}_k)\mathbf{e}(\mathbf{w}_k) \tag{6}$$

where subscript k denotes the iteration step and λ_k is a scalar that controls convergence properties. If λ_k is equal to zero the Levenberg-Marquardt algorithm becomes the Gauss-Newton method. In this study, all BP networks were trained using the Levenberg-Marquardt algorithm with an early-stopping criterion on validation data [42]. This prevented the network from overfitting the training data. All ANN calculations were performed using the Matlab Neural Network Toolbox [43].

3. Application to regular 2D RC frames

The proposed method was applied to predicting seismic damage in analytical models of 2D RC frame structures. Firstly, the procedure was to select a set of suitable parameters that described the properties of the RC frames and ground motions. Secondly, nonlinear FEM analyses of the RC frames were conducted using a suite of ground motion time histories and damage indices calculated that quantified the level of damage caused by the earthquake.

Finally, using the simulation results an ANN was trained to relate the structural and ground motion parameters to the damage index. Once trained, the ANN should be able to predict damage to various other RC frames under different ground motion excitations as described by the input parameters, and this predictive ability was assessed using several numerical examples. The key benefit of the proposed approach is that it formulates a model that allows the prediction of seismic damage in a large class of buildings that may vary in stiffness, strength and topology whilst subjected to a range of different ground motions.

3.1. Structural and ground motion parameters

In this investigation a set of 19 parameters were used for analysis, 13 structural and 6 for ground motion. The structural properties were (i) number of storeys, (ii) number of bays, (iii) the first storey height, (iv) interstorey height for remaining storeys, (v) bay width, (vi) beam depth for first two storeys, (vii) column dimension for first two storeys, (viii) beam depth for remaining storeys, (ix) column dimension for remaining storeys, (x) beam reinforcement ratio, (xi) column reinforcement ratio, (xii) concrete strength and (xiii) damping ratio. Table 1 shows adopted values for parameters (i)-(v) and (x)-(xiii), i.e. frame topology, beam and column reinforcement ratios, concrete strengths, and damping ratios. The 2D RC frames had regular topologies with the number of storeys and bays varying from 3 to 7 and 2 to 4, respectively. The width of all bays in a given frame was assumed equal, however, the first storey was allowed to be higher than the remaining storeys to reflect the topologies often encountered in practice. The appropriate range of an input was either determined by design code recommendations [44] (minimum and maximum reinforcement ratios), typical values reported [45] (damping) or realistic and commonly used dimensions and topologies (bay widths, storey heights and numbers of storeys and bays). Strength of materials, i.e. concrete and steel, were selected based on the practices prevailing in New Zealand, where most of existing building construction uses concrete of compressive strength of either 30 or 40 MPa and Grade 300 steel. Concrete stiffness is commonly estimated based on its compressive strength [44] and this approach was also adopted in this research. (Consequently, steel strength and concrete Young's modulus were not included as variable parameters.)

A number of design rules were implemented for beam and column sizes (structural parameters (vi)-(ix)) to ensure that realistic frames were simulated, and these are summarised in Table 2. The beam depth for the first two storeys is denoted by *d1*, the column depth for the first two storeys *c1*, the beam depth for the remaining storeys *d2*, and the column depth for the remaining storeys *c2*, respectively. All beams were rectangular with width/depth ratio of 2/3, and all columns were square. The columns were assumed wider than the respective beams to allow vertical reinforcement pass through beam-column joints. To allow for realistic variations in section dimensions, the depth of beams for higher storeys was reduced by a fixed amount compared to the first two storeys. For frames with 3 or 4 storeys it was decided to be possible that there could be only one beam size, and consequently column size, and hence Table 2 allows the two beam/column sizes to be equal. For frames with 5 or more storeys it was considered more likely that the lower and upper beam/columns sizes would be different.

The six ground motion parameters were (i) PGA, (ii) PGV, (iii) PGD, (iv) SI, (v) dominant frequency and (vi) effective duration. SI was defined as the average spectral velocity response of a single degree of freedom oscillator with a natural period between T_1 = 0.1s and T_2 = 2.5s and a damping ratio of 20%:

$$\mathrm{SI} = \frac{1}{T_2 - T_1} \int_{T_1}^{T_2} S_V dT \tag{7}$$

where S_V is the spectral velocity and T is the system's natural period [46]. The effective duration of the earthquake was defined as the time over which 90% of the power is released [47]. These parameters have been demonstrated to correlate well with magnitudes of elastic and inelastic structural response indices [26]. To ensure the network learnt the combination of parameters that cause damage, nine earthquake records were used to build the data set. The properties of these earthquakes are given in Table 3.

The simplicity of both the structural and ground motion parameters permits a board range of regular 2D RC frames and ground motions to be described. Additionally, the parameters require no prior structural analysis of the frame, e.g. knowledge of natural period.

3.2. Nonlinear FEM simulations for damage data generation

With the scarcity of complete and accurate historic data, the data sets used in this study were produced from the results of analytical simulations using Ruaumoko [48], a nonlinear FEM structural analysis program. FEM models of frames were constructed by random selection of structural properties from Tables 1 and 2 and running an analysis of each so defined frame for a randomly selected earthquake record from Table 3. Inelastic time-history analyses were performed on all frames using the Newmark Constant Average Acceleration method [45] with parameter $\beta = 0.25$. The Rayleigh proportional damping model was used [45] with the damping ratio taken from Table 1 assigned to the first two modes. The Modified Takeda Hysteretic Rule [49] was used to model the stiffness of the RC members. Yield conditions were calculated based on the appropriate beam/column reinforcement, section dimensions and concrete and steel strength.

Damage in the structure was quantified using the Park and Ang damage index [50]. The damage index D for a particular member can be calculated from

$$D = \frac{\mu_m}{\mu_u} + \frac{\beta E_h}{F_y \mu_u} \tag{8}$$

where μ_m and μ_u are the maximum and ultimate ductilities respectively, E_h is the dissipated hysteretic energy, F_y is the yield action and β is a constant determining the contribution of cyclic loading to the level of damage. In the present study, to assess the global damage to the structure an average of all member damage indices was calculated. From studies on concrete bridge piers, Stone and Taylor [51] proposed a classification of structural damage based on the Park and Ang index. Their classification, shown in Table 4 gives different values of the damage index according to whether the structure was (i) intact or with minor cracking, (ii) reparable, (iii) irreparable, or (iv) collapsed.

3.3. Training and testing of ANN for damage prediction

From the data generation procedure outlined above, a 2819-point data set was obtained with damage indices between $0.05<D<1.2$. This was randomly divided into 2200 points for training and 619 points for testing the ANNs.

Several BP ANN architectures using a single HL and different numbers of HL neurons were investigated. Due to differences in the performance of the networks caused by the selection of initial weights, 50 networks of each configuration were trained. The performance of the network was assessed on the testing data only using the standard deviation of the errors produced by the network, σ_e. The lowest standard deviation obtained for each configuration out of the 50 networks trained is shown in Table 5 together with the number of HL neurons. The table shows good performance over a range of ANN configurations. The network with 20 HL neurons was adopted because it yielded the smallest error standard deviation σ_e=0.042.

The predictive ability of this ANN has been shown graphically in Figure 2 where the damage from FEM analysis has been plotted against damage predicted by the ANN for the testing data. For excellent predictions, the damage predicted by the ANN would equal the FEM value and all data points would sit on the straight, diagonal reference line. The figure shows that the points form along the reference line with some degree of scatter. While most points are close to the reference line, which is consistent with the small value of error standard deviation, a number of outliers can also be seen, where errors are bigger. A stronger scatter can particularly be observed for damage indices larger than 0.8, where in extreme cases the differences between FEM and ANN predicted values can reach 0.2. Overall, however, the ANN provides a good prediction of seismic damage.

An alternative assessment of the performance of the ANNs can be achieved by recording misclassifications against the Stone and Taylor classification shown in Table 4. The output of the ANN shown in Figure 2 was classified into the four classes of observable damage. Using this classification the ANN correctly classified 548 points out of 619 or provided 88.5% of correct classifications. This again can be considered as a good result.

3.4. Assessment of generalisation capabilities of ANNs

One of the strengths of ANNs is their ability to use the learnt relationships to predict outcomes in previously unseen cases. In this section, these abilities are illustrated using three examples in which the BP ANN trained previously is applied to several seismic damage prediction tasks and the results compared against FEM.

In the first example, 5-storey by 3-bay frames with varying beam reinforcement ratios were subjected to the Imperial Valley earthquake with a PGA scaled between 0.20g-0.60g. The nature of extension and challenge was that during the training phase the ANN could only learn the frame damage caused by the original unscaled earthquake and had to apply the learnt knowledge of other earthquake effects to make predictions. PGV, PGD and SI of the ground motion were scaled accordingly, while dominant frequency and effective duration remained unchanged. The structural properties were set as follows: 4.0m 1st storey height, 3.5m interstorey height, 6.0m bay width, 0.020 column reinforcement ratio, 30MPa concrete strength and 5% damping. The section dimensions were: $d1$ = 0.6m, $c1$ = 0.7m, $d2$ = 0.55m and $c2$ = 0.65m. Four different frames were analysed for which the beam reinforcement ratio assumed the different values listed in Table 1, while column reinforcement ratio was constant p=0.020. The inputs were presented to the ANN trained above and the results were compared with those obtained from FEM analysis, see Figure 3. The figure shows generally good agreement over the range of medium PGA values. For p=0.008 this range is from 0.313g to 0.55g, for p=0.012 and 0.016 from 0.313g to 0.60g, and for p=0.020 from 0.35g to 0.60g. Larger errors were observed for smaller and larger PGA outside these ranges. For all considered reinforcement ratios the ANN overestimated the damage indices for small PGA; for p=0.008 it underestimated them for PGA beyond 0.55g. The largest absolute errors for each considered reinforcement ratio were respectively 0.13, 0.08, 0.06, and 0.04. These errors do not, however, appear to be excessive and could be due to the limited number of earthquake records used in training. Hence it can be concluded that the ANN has successfully applied knowledge about other earthquakes and structures to produce the interpolation shown in the figure.

In the second example, damage was predicted to frames with a previously unseen topology, 4-storeys by 3-bays. All 9 earthquakes were used in the analysis and structural parameters were able to take values shown in Table 1. Section dimensions were able to assume the values shown for the 4-storey by 4-bay frame in Table 2. A data set of 160 points was generated for assessing the performance of the ANN. The results are shown graphically in Figure 4 where the damage obtained from FEM has been plotted against the ANN value. The figure shows the ANN has been successfully able to generalise damage to a previously unseen building topology. The standard deviation of the errors was σ_e=0.062. A majority of the data points were near the reference line with some acceptable degree of scatter. However, a number of poorly predicted cases can also be seen especially for indices larger than 0.6 where in several cases the individual errors were of the order of 0.2 or larger.

In the third example, the ANN was used to predict damage to all frame topologies caused by a previously unseen earthquake. The Coalinga 1983 earthquake was chosen and the properties of this record are shown in Table 6. A data set of 225 points was generated. The results are shown graphically in Figure 5 in the same format as above. There was clearly much more scatter than in previous examples with error standard deviation σ_e=0.104. Extreme individual errors were of the order of 0.3 or larger. The ANN also appeared to be under conservative.

4. Conclusions

In this study, an alternative to seismic vulnerability curves for assessing damage to groups of structures was proposed. The proposed method used ANNs to model a relationship between parameters describing both the structure and ground motion and damage. The approach was to describe both the structure and ground motion using a large number of structural and ground motion properties. The class of structures analysed were 2D RC frames with varying topology, stiffness, strength and damping, and subjected to a suite of ground motions. Using the results of FEM simulations, a mapping between the structural and ground motion properties and the damage indices was established using an ANN. The performance of the ANN was assessed using several examples and the ANN was found to be capable of successfully predicting damage. The errors between FEM and ANN results were on average acceptable but a relatively large number of significantly different damage predictions could also be observed. The case of predictions for a previously unseen earthquake proved to be particularly challenging in this respect. Because of the nature of ANNs which learn relationships by example the applicability of their proposed particular implementation is limited to the range of parameters, such a topologies, material properties etc., used in training. The ANN has been demonstrated to interpolate the learnt relationship within that range but any extension will require the generation of additional training data over an appropriately expanded parameter range.

The proposed approach to seismic-induced damage prediction would be beneficial for both hypothetical earthquake scenarios and post-earthquake damage evaluation, as it would enable quick prediction of building damage. To expand the method's applicability, further studies may include more inputs and investigate more realistic and complex structures. A potential drawback of the approach is the generation of data sets which is time consuming and more efficient ways of generating training data will need to be investigated.

References

[1] Ramos LF, Lourenco PB. Modeling and vulnerability of historical city centers in seismic areas: A case study in Lisbon. Engineering Structures 2004; 26: 1295-310.

[2] Elnashai AS. Analysis of the damage potential of the Kocaeli (Turkey) earthquake of 17 August 1999. Engineering Structures 2000; 22: 746-54.

[3] Magliulo G, Fabbrocino G, Manfredi G. Seismic assessment of existing precast industrial buildings using static and dynamic nonlinear analyses. Engineering Structures 2008; 30: 2580-8.

[4] Chi W-M, El-Tawil S, Deierlein GG, Abel JF. Inelastic analyses of a 17-story steel framed building damaged during Northridge. Engineering Structures 1998; 20: 481-95.

[5] Jeong S-H, Elnashai AS. Probabilistic fragility analysis parameterized by fundamental response quantities. Engineering Structures 2007; 29: 1238-51.

[6] Kwon O-S, Elnashai A. The effect of material and ground motion uncertainty on the seismic vulnerability curves of RC structure. Engineering Structures 2006; 28: 289-303.

[7] Benedetti D, Benzoni G, Parisi MA. Seismic vulnerability and risk evaluation for old urban nuclei. Earthquake Engineering and Structural Dynamics 1988; 16: 183-201.

[8] Hassan AF, Sozen MA. Seismic vulnerability assessment of low-rise buildings in regions with infrequent earthquakes. ACI Structural Journal 1997; 94: 31-9.

[9] Dowrick DJ, Rhoades DA, Davenport PN. Damage ratios for domestic property in the magnitude 7.2 1968 Inangahua, New Zealand, earthquake. Bulletin of the New Zealand Society for Earthquake Engineering 2001; 34: 191-213.

[10] Rossetto T, Elnashai A. Derivation of vulnerability functions for European-type RC structures based on observational data. Engineering Structures 2003; 25: 1241-63.

[11] Lagomarsino S, Podestá S. Seismic vulnerability of ancient churches: II. Statistical analysis of surveyed data and methods for risk analysis. Earthquake Spectra 2004; 20: 395-412.

[12] Dolce M, Kappos A, Masi A, Penelis G, Vona M. Vulnerability assessment and earthquake damage scenarios of the building stock of Potenza (southern Italy) using Italian and Greek methodologies. Engineering Structures 2006; 28: 357-71.

[13] Li Q, Ellingwood BR. Damage inspection and vulnerability analysis of existing buildings with steel moment-resisting frames. Engineering Structures 2008; 30: 338-51.

[14] D'Ayala D, Spence R, Oliveira C, Pomonis A. Earthquake loss estimation for Europe's historic town centres. Earthquake Spectra 1997; 13: 773-92.

[15] Calvi GM. A displacement-based approach for vulnerability evaluation of classes of buildings. Journal of Earthquake Engineering 1999; 3: 28.

[16] Dymiotis C, Kappos AJ, Chryssanthopoulos MK. Seismic reliability of RC frames with uncertain drift and member capacity. Journal of Structural Engineering 1999; 125: 1038-47.

[17] Dymiotis C, Kappos AJ, Chryssanthopoulos MK. Seismic reliability of masonry-infilled RC frames. Journal of Structural Engineering 2001; 127: 296-305.

[18] Porter KA, Kiremidjian AS, LeGure JS. Assembly-based vulnerability of building and its use in performance evaluation. Earthquake Spectra 2001; 17: 291-312.

[19] Lang K, Bachmann H. On the seismic vulnerability of existing buildings: A case study of the city of Basel. Earthquake Spectra 2004; 20: 43-66.

[20] Choi E, DesRoches R, Nielson B. Seismic fragility of typical bridges in moderate seismic zones. Engineering Structures 2004; 26: 187-99.

[21] Rossetto T, Elnashai A. A new analytical procedure for the derivation of displacement-based vulnerability curves for populations of RC structures. Engineering Structures 2005; 27: 397-409.

[22] Borzi B, Pinho R, Crowley H. Simplified pushover-based vulnerability analysis for large-scale assessment of RC buildings. Engineering Structures 2008; 30: 804-20.

[23] Erberik MA. Fragility-based assessment of typical mid-rise and low-rise RC buildings in Turkey. Engineering Structures 2008; 30: 1360-74.

[24] Serdar Kircil M, Polat Z. Fragility analysis of mid-rise R/C frame buildings. Engineering Structures 2006; 28: 1335-45.

[25] Elenas A, Meskouris K. Correlation study between seismic acceleration parameters and damage indices of structures. Engineering Structures 2001; 23: 698-704.

[26] Riddell R. On ground motion intensity indices. Earthquake Spectra 2007; 23: 147-73.

[27] Yücemen MS, Özcebe G, Pay AC. Prediction of potential damage due to severe earthquakes. Structural Safety 2004; 26: 349-66.

[28] Yakut A, Özcebe G, Yücemen MS. Seismic vulnerability assessment using regional empirical data. Earthquake Engineering and Structural Dynamics 2006; 35: 1187–202.

[29] Adeli H. Neural networks in civil engineering: 1989-2000. Computer-Aided Civil and Infrastructure Engineering 2001; 16: 126-42.

[30] Wu X, Ghaboussi J, Garrett JH. Use of neural networks in detection of structural damage. Computers and Structures 1992; 42: 649-59.

[31] Nakamura M, Masri SF, Chassiakos AG, Caughey AK. A method for non-parametric damage detection through the use of neural networks. Earthquake Engineering and Structural Dynamics 1998; 27: 997-1010.

[32] Zang C, Imregun M. Structural damage detection using artificial neural networks and measured FRF data reduced via principal component projection. Journal of Sound and Vibration 2001; 242: 813-27.

[33] Molas GL, Yamazaki F. Neural networks for quick earthquake damage estimation. Earthquake Engineering and Structural Dynamics 1995; 24: 505-16.

[34] De Stefano A, Sabia D, Sabia L. Probabilistic neural networks for seismic damage mechanisms prediction. Earthquake Engineering and Structural Dynamics 1999; 28: 807-21.

[35] Aoki T, Ceravolo R, De Stefano A, Genovese C, Sabia D. Seismic vulnerability assessment of chemical plants through probabilistic neural networks. Reliability Engineering and System Safety 2002; 77: 263-8.

[36] Erkus B. Utilization of artificial neural networks in building damage prediction. Middle East Technical University, Ankara, Turkey, 1999.

[37] Sánchez-Silva M, García L. Earthquake damage assessment based on fuzzy logic and neutral networks. Earthquake Spectra 2001; 17: 89-112.

[38] Anderson JA, Rosenfeld E, editors. Neurocomputing: Foundations of research, Cambridge, Massachusetts: MIT Press, 1988.

[39] Rumelhart DE, Hinton GE, Williams RJ, Learning internal representations by error propagation, in Parallel distributed processing: Explorations in the microstructures of cognition, Rumelhart DE, McClelland JL, editors. 1986, MIT Press: Cambridge, Massachusetts. 318-62.

[40] Hagan MT, Demuth HB, Beale MH. Neural network design, Boston, Massachusetts: PWS Pub., 1996.

[41] Marquardt D. An algorithm for least squares estimation of nonlinear parameters. Journal of the Society for Industrial and Applied Mathematics 1963; 11: 431-41.

[42] Howard D, Beale M, Hagan M. Neural network toolbox: User's guide version 4., Natick, Massachusetts: Mathworks, 2005.

[43] Demuth HB, Beale MH, Hagan MT. Neural network toolbox 5: User's guide, Natick, M.A.: Mathworks, 2006.

[44] Standards New Zealand. NZS 3101:1995 concrete structures standard, Wellington: Standards New Zealand, 1995.

[45] Chopra AK. Dynamics of structures: Theory and applications to earthquake engineering, 2nd ed, Upper Saddle River, New Jersey: Prentice Hall, 2001.

[46] Katayama T, Sato N, Saito K. SI-sensor for the identification of destructive earthquake ground motion, in The 9th World Conference on Earthquake Engineering, Tokyo and Kyoto, 1988, 667-72.

[47] Trifunac MD, Brady AG. A study on the duration of strong earthquake ground motion. Bulletin of the Seismological Society of America 1975; 68: 1487–520.

[48] Carr AJ. Ruaumoko - program for inelastic dynamic analysis, Christchurch: Department of Civil Engineering, University of Canterbury, 1998.

[49] Otani S. Sake, a computer program for inelastic response of R/C frames to earthquakes. UILU-Eng-74-2029, University of Illinois, Urbana-Champaign, Illinois, 1974.

[50] Park YJ, Ang AH. Mechanistic seismic damage model for reinforced concrete. Journal of Structural Engineering, ASCE 1985; 111: 722-39.

[51] Stone WC, Taylor AW. Seismic performance of circular bridge columns designed in accordance with AASHTO/CALTRANS standards, Gaithersburg MD, 1993.

Figure 1

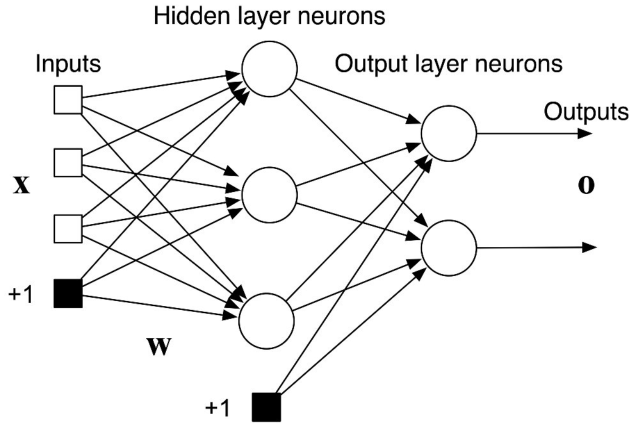

Figure 1. Structure of a single hidden layer BP ANN.

Figure 2

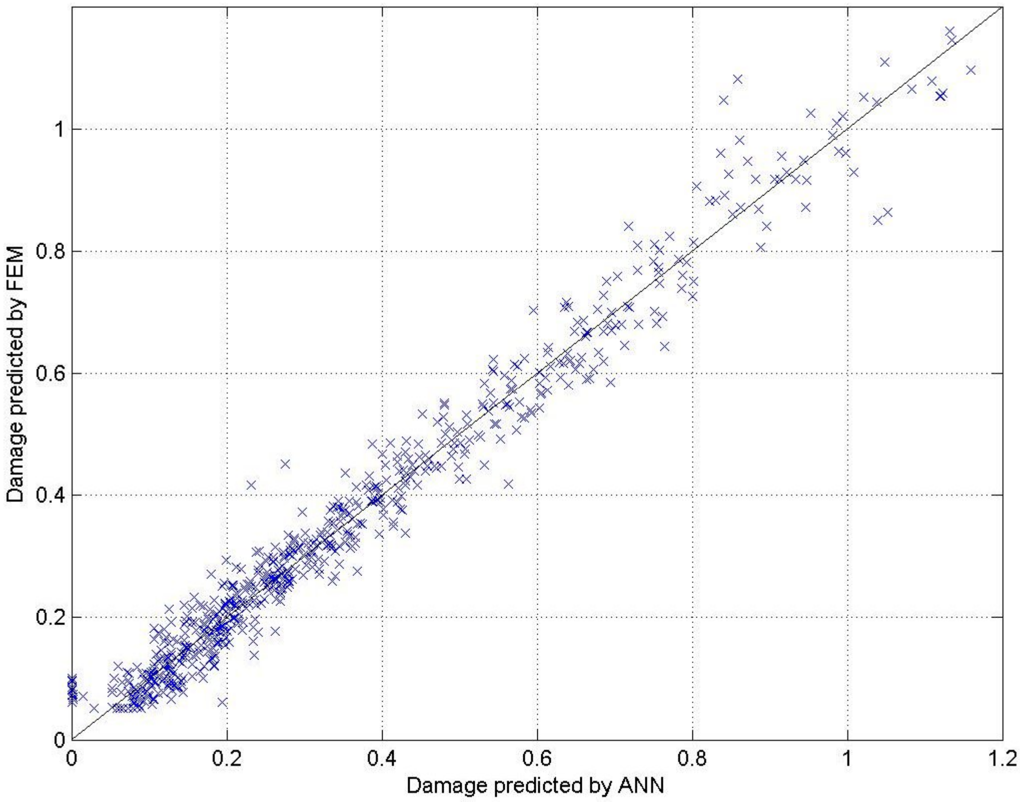

Figure 2. Comparison of damage predicted by FEM and ANN.

Figure 3

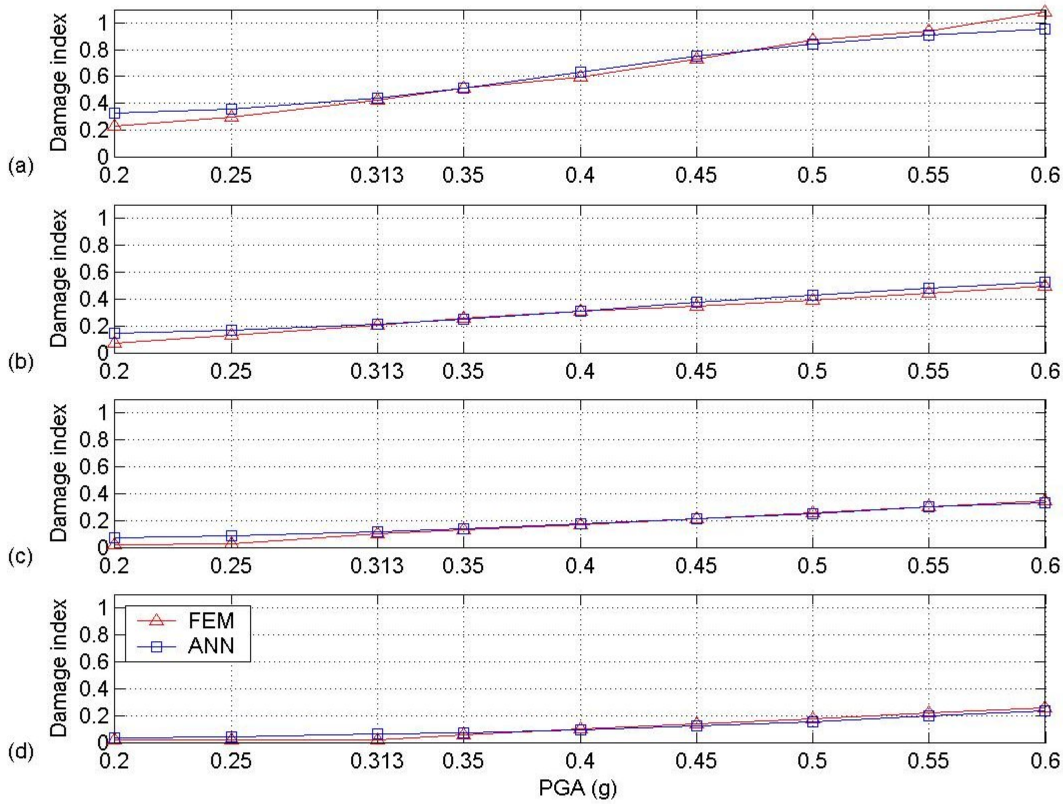

Figure 3. Comparison of damage predicted by FEM and ANN caused by scaled Imperial Valley earthquake to 5-storey by 3-bay frames with varying beam reinforcement ratio: (a) p = 0.008, (b) p = 0.012, (c) p = 0.016, and (d) p = 0.020.

Figure 4

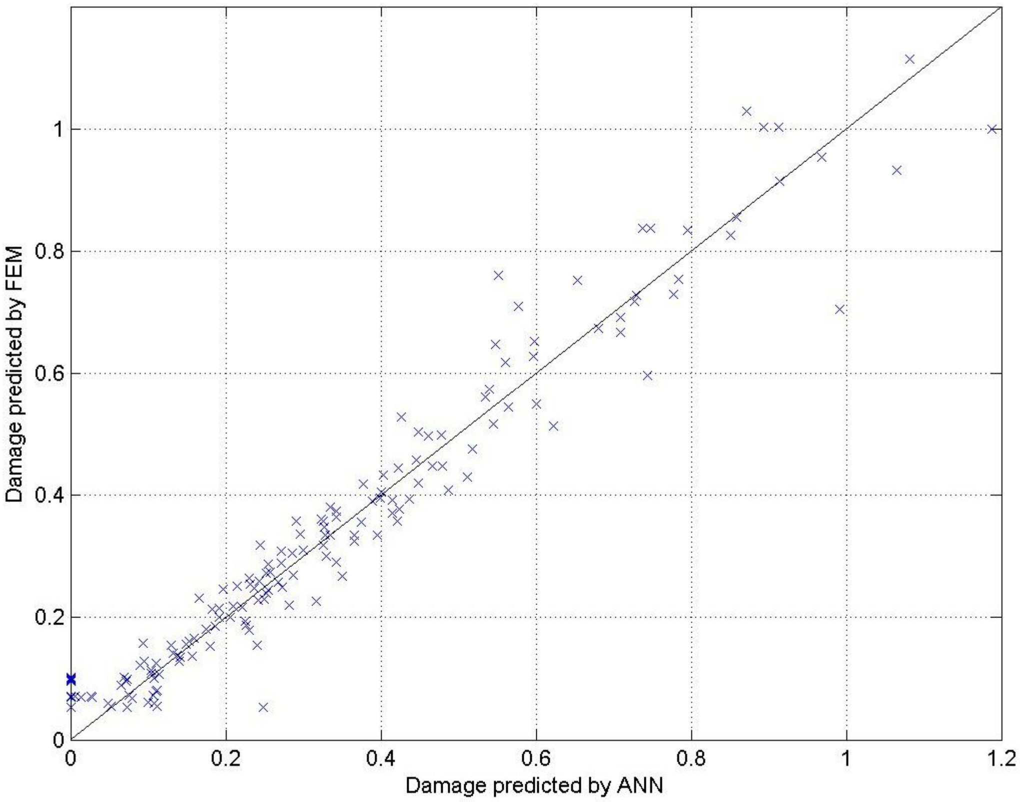

Figure 4. Comparison of damage predicted by FEM and ANN to a 4-storey by 3-bay frame.

Figure 5

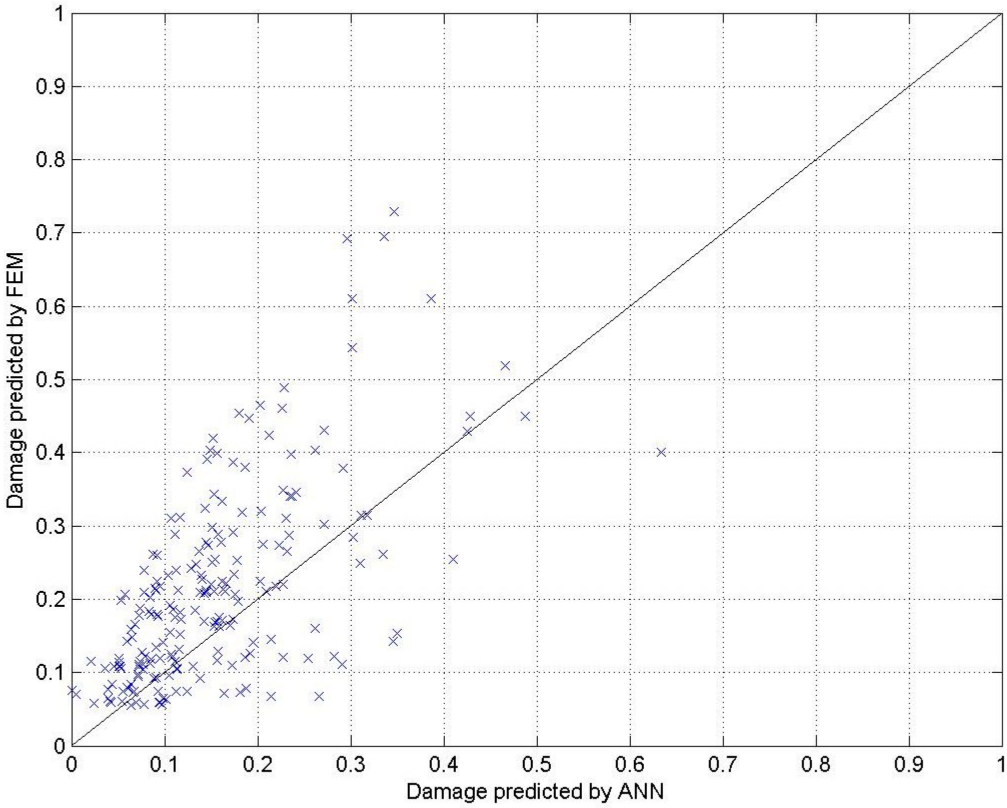

Figure 5. Comparison of damage predicted by FEM and ANN caused by Coalinga earthquake.

Table 1. Frame topologies, beam and column reinforcement ratios, concrete strengths, and damping rations used in numerical simulations.

Parameter	Adopted values
1st storey height (m)	3.0, 3.5, 4.0 or 4.5[a]
Remaining storey height (m)	3.0, 3.5 or 4.0
Bay width (m)	5.0, 6.0 or 7.0
Beam reinforcement ratio	0.008, 0.012, 0.016 or 0.020
Column reinforcement ratio	0.010, 0.020, 0.030, 0.040 or 0.050
Concrete strength (MPa)	30 or 40
Damping ratio (%)	2 or 5

[a] Must be greater than or equal to remaining storey height (2nd row).

Table 2. Beam and column dimensions for different frame topologies.

	Type (storeys × bays)		
Parameter	3×2, 3×3, 3×4 and 4×4	5×3 and 5×4	6×3 and 7×4
d1 (m)	0.4, 0.45, 0.5 or 0.55	0.5, 0.55, 0.6 or 0.65	0.55, 0.6, 0.65 or 0.70
c1 (m)	*d1* + 0.1	*d1* + 0.1	*d1* + 0.1
d2 (m)	*d1* or *d1* – 0.05	*d1* – 0.05 or *d1* – 0.075	*d1* – 0.05 or *d1* – 0.075
c2 (m)	*d2* + 0.1	*d2* + 0.1	*d2* + 0.1

Table 3. Properties of earthquakes used in numerical simulations.

Earthquake	PGA (g)	PGV (cm/s)	PGD (cm)	SI (cm/s)	Dominant freq. (Hz)	Effective duration (s)
Duzce 12/11/1999	0.535	83.5	51.6	135	1.17	10.8
Erzincan 13/3/1992	0.496	64.3	22.8	132	1.56	7.35
Gazli 17/5/1976	0.718	71.6	23.7	127	3.32	6.84
Helena 31/10/1935	0.173	16.5	2.37	23.0	0.98	2.25
Imperial Valley 19/5/1940	0.313	29.8	13.3	68.4	1.17	24.1
Kobe 17/1/1995	0.345	27.6	9.60	71.2	0.59	12.9
Loma Prieta 18/10/1989	0.472	33.9	8.00	60.6	2.54	3.68
Northridge 17/1/1994	0.568	52.1	4.21	99.4	1.22	9.08
Taiwan 20/5/1986	0.172	33.0	6.94	68.4	0.68	13.0

Table 4. Classification of structural damage based on the Park and Ang damage index.

Damage index value	Qualitative damage description
$D<0.11$	No damage or localised minor cracking
$0.11 \leq D<0.4$	Repairable – extensive spalling but inherent stiffness remains
$0.4 \leq D<0.77$	Irreparable – still standing but failure imminent
$D \geq 0.77$	Collapsed

Table 5. Standard deviation of errors produced by ANNs with different number of HL neurons.

HL neurons	6	8	10	12	14	16	18	20	22	24
Standard deviation	0.078	0.068	0.059	0.052	0.057	0.055	0.046	0.042	0.045	0.055

Table 6

Table 6. Coalinga earthquake properties.

Earthquake	PGA (g)	PGV (cm/s)	PGD (cm)	SI (cm/s)	Dominant freq. (Hz)	Effective duration (s)
Coalinga 22/07/1983	0.408	18.9	5.64	40.7	0.781	14.1